Research on Data-Driven Dynamic Reconfiguration and Energy-Saving Optimization Methods for Building Energy-Consuming Microgrids

Shengli Liu[1], Dantong Liu[2]
[1]Jinan Government-Subsidized Housing Service Center, Jinan 250001, Shandong, China
[2]Engineering Division Five, Jinan City Construction Group, Jinan 250001, Shandong, China
Corresponding author: Shengli Liu (e-mail: sdjnlslok@163.com)

ABSTRACT This study proposes a data-driven dynamic reconfiguration and energy-saving optimization framework for building energy-consuming microgrids. By integrating multi-source sensing data, load forecasting, and dynamic topology optimization, the framework establishes a coupling mechanism between building energy consumption and microgrid operation. A hierarchical architecture consisting of data acquisition, intelligent prediction, optimization decisionmaking, and execution control is developed to support adaptive energy management under varying load conditions. Load forecasting is performed using a long short-term memory network, while an enhanced particle swarm optimization algorithm is employed to determine optimal microgrid reconfiguration strategies under operational constraints. Case studies based on commercial building scenarios demonstrate that the proposed framework effectively improves load regulation capability, enhances renewable energy utilization, and supports stable microgrid operation. The framework can be readily integrated with wireless sensing infrastructures, antenna-enabled monitoring platforms, and edge–cloud collaborative systems, providing an engineering-oriented solution for real-time energy management and intelligent microgrid optimization in modern building environments.

INDEX TERMS building microgrid, dynamic reconfiguration, energy-saving optimization, wireless sensing systems

I. INTRODUCTION

A. RESEARCH BACKGROUND AND SIGNIFICANCE

WITH the accelerated pace of global urbanization, the building sector—a major energy consumer—continues to see rising energy consumption. According to an authoritative 2024 report by the International Energy Agency (IEA), global building energy consumption accounts for a staggering 39% of total energy use, underscoring the sector's significant role in energy consumption. In China, building energy consumption is equally substantial, accounting for 28.7% of the nation's total energy use. This significant share underscores the critical role of building energy management within the national energy strategy [1].

Traditional power grids operate under a "centralized generation-long-distance transmission-passive consumption" model, which faces numerous challenges in addressing the rapid growth of building energy consumption. Firstly, significant load fluctuations have become a prominent issue. In commercial buildings, air conditioning systems—the primary energy-consuming equipment—account for an extremely high proportion of the load, causing electricity demand to fluctuate dramatically between day and night and across seasons. Industrial parks, due to variations in production processes, experience peak-to-off-peak differences exceeding 3:1, further exacerbating grid load imbalance. Such load fluctuations not only increase the difficulty of grid dispatch but may also lead to frequent equipment start-ups and shutdowns, reducing equipment lifespan and increasing operation and maintenance costs.

B. RESEARCH CONTENT

A core focus of this research is developing a building energy consumption-microgrid coupling model. This model aims to comprehensively describe the interactive relationship between building energy consumption and microgrid operation, providing theoretical support for dynamic reconfiguration. During development, it is essential to integrate the building's physical characteristics, the operating modes of energy-consuming equipment, and the microgrid's topology and control strategies. By establishing a detailed mathematical model, the energy consumption of the building and the operational status of the microgrid can be simulated under various scenarios, providing an accurate data foundation for subsequent load forecasting and dynamic reconfiguration [2].

Specifically, the building energy consumption model must encompass the energy characteristics of primary systems such as HVAC, lighting, and power equipment, while accounting for external factors like ambient temperature, humidity, and light intensity that influence energy usage. The microgrid model must describe energy flow relationships among distributed power sources, energy storage devices, loads, and the grid, along with the impact of control strategies on system operation. Coupling the building energy consumption model with the microgrid model creates a comprehensive system model for analyzing the dynamic relationship between building energy consumption and microgrid operation [3].

II. ANALYSIS OF COUPLING MECHANISMS BETWEEN BUILDING ENERGY CONSUMPTION AND MICROGRIDS

A. MODELING BUILDING ENERGY CONSUMPTION CHARACTERISTICS

1) Analysis of Energy Consumption Composition

The accurate study of building energy usage is the foundation of building a coupling model of building energy use and microgrids. One of the commercial complexes that were chosen as the study object is a representative one in Beijing. This complex is also based in the center of the commercial part of Beijing, in the Chaoyang District, which combines shopping, office, dining, and entertainment capabilities, measuring 128,000 square meters. The data on its energy consumption derives out of 12 months of continuous monitoring records (captured through Building Automation System (BAS)) in real-time (July 2022 - June 2023) and with a sampling frequency of 15 minutes. The data has a high completeness rate of 99.2 per cent which is degree of authenticity and reliability is high [4].

Based on the analytical mining and detailed study of the data related to the energy consumption of this commercial complex, the distribution of energy consumption according to the categories is indicated in Table 1. In the table, it is obvious that the HVAC system consumes the largest portion of the building's energy, accounting for 58.3% of the total annual consumption. Furthering into the reasons, being a densely populated facility, the complex has the peak of foot traffic reaching tens of thousands of visitors every day. The air conditioning system should be able to function during long hours to achieve a comfortable indoor environment by fulfilling the physiological and psychological needs of the consumers and office workers. One can notice that during hot summer periods much more often than not, Beijing as a destination faces temperatures that are far over 35°C (95°F). The cooling load of the air conditioning system shoots up exponentially to sustain the indoor temperatures of the comfortable range of 24–26°C (75–79°F). When the outdoor temperature may reach -10°C in winter, heating systems are required to work at full capacity so as to keep the indoor temperatures higher than 20°C. Statistics indicate that air conditioning energy use represents approximately 60% of all monthly energy use during the hottest summer months (July–August); and even during the coldest winters (December–January) this percentage remains close to 60%, aligning with the annual average contribution of the HVAC system.

TABLE 1. Commercial Complex Energy Consumption Breakdown

Energy Type	Energy Consumption Percentage (%)
HVAC System	58.3
Lighting System	22.1
Equipment & Sockets	15.2
Other Energy Consumption	4.4

The high consumption of lighting systems is 22.1%. The lighting specifications of commercial complexes are extremely dynamic and various as they involve not only the regular operational light, as it includes display lights in the retail stores and simple light along corridors, but there is also the emergency lighting that is needed in case of an emergency to make sure people can safely evacuate the complex, and the decorative lighting that would give the complex its unique retailing atmosphere [5]. Moreover, commercial complexes work long hours, during which they generally operate 10:00 AM to 10:00 PM and other entertainment spots do not close till the early hours. Such updated lighting operation also leads to constantly high energy consumption. An example is a huge clothing store in a shopping center that will utilize several banks of powerful spotlights in the display lighting, which will be open all day (12 hours a day). One retail outlet can use hundreds of kilowatt-hours of lighting power in a month.

The energy usage of the equipment outlet makes 15.2%. This category encompasses the power consumption of office equipment, elevators, escalators and other electrical facilities. Commercial complexes include hundreds of office compartments with enormous numbers of computers, printers, copiers and other office devices with some in standby position 24/7 to constantly use electricity. It has elevators and escalators that are key means of transporting passengers vertically with extremely high frequencies. It is calculated that the 20 elevators and 15 escalators contained within this commercial complex account for a combined cumulative total of more than 100 operating hours per day, representing a significant source of energy consumption. The other energy consumption amounts to 4.4, which mainly consists of water provision and drainage systems, firefighting water and fire fighting equipments etc., which inevitably require electrical power for their operation [6]. The fact that fire protection equipment is kept in the standby state during regular periods does not mean that it does not need constant power as a way of monitoring and maintaining its equipment thus necessitating some level of energy consumption. The distribution of energy consumption is shown in Figure 1:

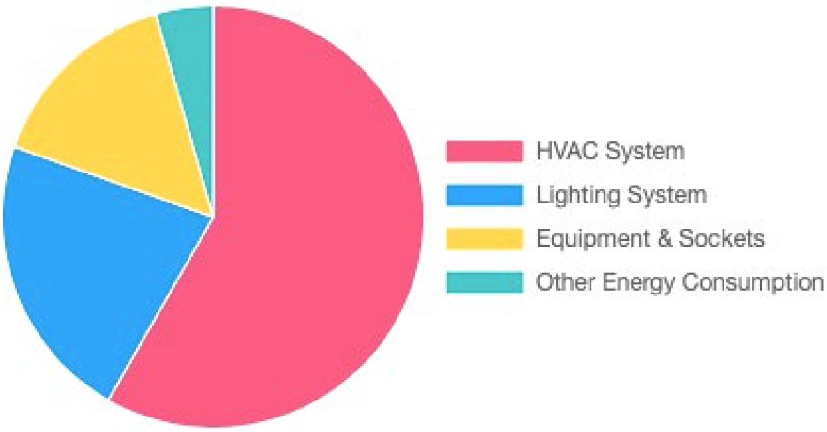

FIGURE 1. Energy Consumption Distribution

The daily fluctuation coefficient reflects the variation of each energy consumption type across different time periods within a day. The daily fluctuation coefficient for the air conditioning system is 1.8, indicating significant load changes throughout the day. For example, during daytime peak operating hours, increased human activity raises indoor thermal loads, requiring the air conditioning system to boost cooling or heating capacity, leading to higher energy consumption. Conversely, during nighttime non-operating hours, the air conditioning load decreases substantially. The daily fluctuation coefficient for the lighting system is 1.2, primarily influenced by operating hours [7]. Lighting demand remains relatively stable during daytime, while partial area lighting is turned off at night, reducing energy consumption. The daily fluctuation coefficients for plug loads and other miscellaneous energy categories remain near 1.0, suggesting relatively stable demand throughout the 24-hour cycle.

Seasonal fluctuation coefficients reflect variations across energy consumption types during different seasons. The air conditioning system exhibits a high seasonal fluctuation coefficient of 3.2, with peak usage occurring during summer and winter, significantly increasing energy consumption [8]. Conversely, spring and autumn feature more moderate climates, reducing air conditioning frequency and corresponding energy usage. The lighting system maintains a seasonal fluctuation coefficient of 1.0, indicating minimal seasonal impact on its energy consumption. The seasonal fluctuation coefficient for equipment outlets is 1.1, likely due to variations in equipment usage driven by differing levels of commercial activity across seasons. Other energy consumption categories also exhibit a seasonal fluctuation coefficient of 1.0, indicating they remain largely stable [9].

2) Dynamic Characteristics Analysis

Building energy consumption exhibits distinct dynamic characteristics, revealing different patterns of change across varying time scales. In-depth analysis of these dynamic properties is crucial for accurately forecasting building energy demand and enabling dynamic reconfiguration of microgrids.

On a daily scale, using this commercial complex as an example: Conversely, the period from 23:00 to 07:00 the following day constitutes the off-peak period. During this time, the complex largely ceases operations, occupancy is minimal, and air conditioning load drops significantly [10]. The peak load during this period is 2.8 times the off-peak load. These daily load fluctuations pose challenges to the power supply stability of the microgrid, necessitating dynamic reconfiguration to reasonably adjust power supply strategies.

Figure 2 illustrates the typical daily HVAC load curve for this commercial complex. The graph clearly shows the load fluctuations throughout the day, peaking around 14:00 before gradually declining.

On a seasonal scale, summer and winter represent peak periods for building energy consumption, while spring and autumn exhibit relatively lower energy usage. During summer, high temperatures significantly increase cooling demands, driving overall energy consumption upward. In winter, cold weather necessitates the operation of heating systems and heating equipment, maintaining energy consumption at elevated levels. Calculations indicate that peak summer loads are approximately 1.2 times higher than peak winter loads. This ratio is mathematically consistent with the finding that HVAC systems account for a similar proportion of energy use in both seasons (approximately 58.3% to 62%). While the HVAC system remains the dominant consumer year-round, the slightly higher summer total is primarily driven by the cumulative effect of high outdoor temperatures and internal heat gains from lighting and equipment, which increase the cooling cooling load, whereas in winter, internal heat gains partially offset the heating demand. This seasonal variance, while the HVAC system maintains a dominant share in both seasons, is primarily attributed to the lower energy efficiency of cooling cycles compared to heating recovery, coupled with increased internal heat gains from high-intensity lighting and dense

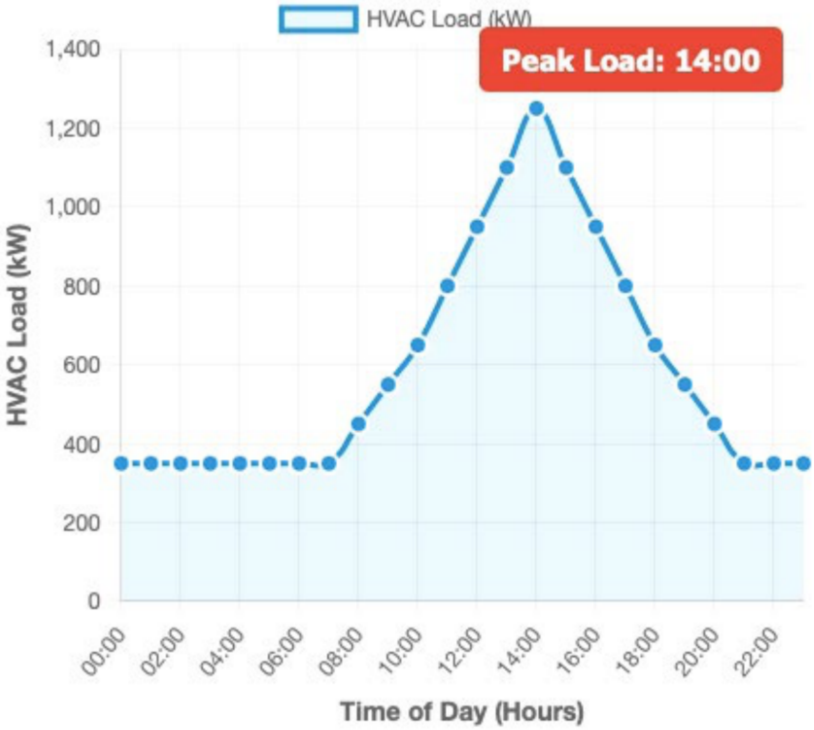

FIGURE 2. -Day HVAC Load Analysis for Commercial Complex

occupancy during summer months, which further amplifies the cooling requirement [11].

B. PHYSICAL BASIS FOR MICROGRID RECONFIGURATION

1) Topological Structure Classification

Topology plays a vital role in the performance of the microgrid. The most typical microgrid topologies are radial, ring and mesh topologies, which have their own advantages, disadvantages and applications. Radial topology is applicable for the small building complex. The topology represents the radiation of power supply from central node to the surrounding load nodes. It is like the branches of a tree which come out of the trunk. Its advantages are simplicity and low line losses, because the current flows from central node to load nodes, so the energy dissipation does not take place in the intermediate segments [12]. Disadvantage of radial topology is that it has low reliability. If any failure occurs at central node or any supply line, the power outage range will be all the loads connected at that line and the area is very wide.

Ring topology is used in the industrial parks. All the load nodes are connected into a closed loop and the power can be introduced from any point of the ring. The reliability of ring structures is high. If any line gets failed, the load can be transferred to the other available lines by the switching equipment, so the power supply will not be interrupted [13]. Ring structures are difficult to control, so the power flow calculation should be accurate and the protection schemes should be coordinated to avoid the circulating current and overload failures. Mesh topology is used in the urban complexes. It has multiple power and load nodes and a large number of connecting lines which construct the complicated mesh structure. The mesh topology has highest flexibility, the topology of the whole structure can be adjusted according to the actual demand of power and load, so it can adjust the supply path reasonably to get the balance of energy distribution. The reliability of mesh structure is also very high. Even if any line or node fails, it will not cause much impact on the whole power supply. Disadvantage of mesh structure is that the investment is high, the requirement of technology for construction and maintenance is high.

2) Constraints for Dynamic Reconfiguration

Multiple constraints must be considered during microgrid dynamic reconfiguration to ensure safe, stable, and economical operation.

Voltage constraints represent a critical factor. According to national standards and relevant specifications, microgrid voltage must remain within the range of 380V $\pm$ 5%. Voltage levels that are too high or too low can disrupt the normal operation of electrical equipment and may even cause damage [14].

Power flow constraints require line load factors to remain below 80%. Line load factor refers to the ratio of actual transmitted power to the line's rated capacity. Excessive load factors increase line heating, accelerate aging, and may trigger safety incidents. Additionally, high load factors limit the microgrid's power transmission capacity and degrade power supply quality. During dynamic reconfiguration, power must be allocated reasonably based on load forecasts and line transmission capabilities to prevent line overloading. Figure 3 illustrates the load rate variations of a specific line across different time periods. It is evident that during certain periods, the line load rate approaches or exceeds 80%, necessitating reconfiguration adjustments.

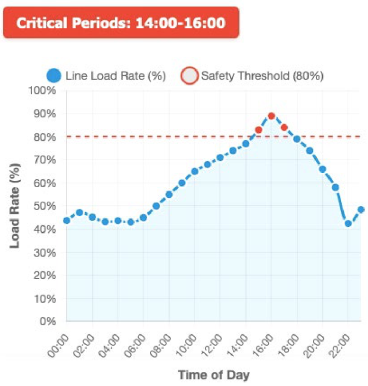

FIGURE 3. -Line Load Rate Analysis

Regarding renewable energy constraints, to ensure stable microgrid operation and power quality, the photovoltaic penetration rate should remain below 40%. This rate represents the ratio of photovoltaic power generation to the total microgrid load power [15].

Figure 4 illustrates power fluctuations in microgrids under varying PV penetration rates. It is evident that as PV penetration increases, the magnitude of power fluctuations progressively grows.

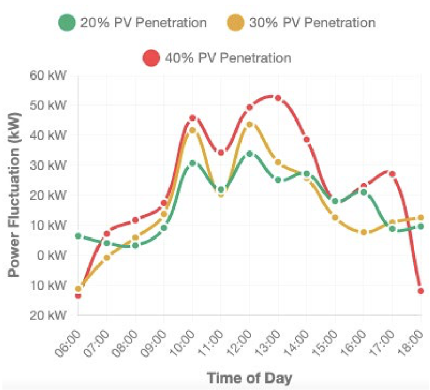

FIGURE 4. Impact of PV Penetration on Microgrid Power Fluctuation

C. DATA-DRIVEN RECONSTRUCTION FRAMEWORK

1) Data Acquisition Layer

The given table lists three classes of sensors which are smart meters, temperature sensors and humidity sensors, the parameters measured by them, sample rates, the degree of accuracy and their uses. Smart meters are also set to measure current, voltage, active power, and reactive power with a very high sampling rate of 1 second. A precision of Class 0.5S provides them with good results in monitoring of equipment-level of energy. It is an accurate and high-frequency measurement that makes the electrical consumption behavior of individual systems or devices more detailed [16]. Through constant monitoring of these parameters, facilities will be able to detect unnecessary and energy wasting equipment, streamline use of power and lower use of electricity.

The temperature sensors should be able to optimize the HVAC (Heating, Ventilation, and Air Conditioning) control; to do this, the sensors need to have a sampling interval of 30 seconds and a $\pm 0.5°C$ accuracy. Such a relatively common sampling allows the system to react timely to changes in temperature in both the house and the outside. The accuracy will be high which means that the occupants will be comfortable and the HVAC system will not be contributing to energy wastage as it keeps the target temperatures accurate.

Humidity detectors with a sampling interval every 30 seconds and a percentage RH accuracy of up to $+3\%$ are crucial in ensuring there is an ideal humidity level of the indoors. Human health needs to be well-hydrated to avoid the development of mold and bacteria as well as to preserve building materials and equipment. These sensors aid in the modification of the ventilation system and dehumidification system by measuring the humidity correctly to achieve an indoor setting that is healthy and comfortable [17]. In general, these sensors collaborate to achieve efficiency in using energy, indoor air quality, and facilitate smart building and facility functioning. The detailed information of data collection is shown in Table 2:

TABLE 2. Data Collection Details

Sensor Type	Measured Parameters	Sampling Rate	Accuracy
Smart Meter	Current, Voltage, Active Power, Reactive Power	1 second	Class 0.5S
Temperature Sensor	Indoor/Outdoor Temperature	30 seconds	$\pm 0.5°C$
Humidity Sensor	Indoor/Outdoor Humidity	30 seconds	$\pm 3\%$ RH

Figure 5 illustrates the installation diagram of the smart meter and temperature/humidity sensors, along with sample collected data. As shown, the electrical parameters collected by the smart meter and the environmental parameters collected by the temperature/humidity sensors provide an intuitive reflection of the equipment's operational status and environmental conditions.

System-level data collection is achieved through the Building Automation System (BAS) and the PV inverter SCADA system. The BAS enables centralized monitoring and management of various building equipment, including HVAC systems, ventilation systems, and water supply/drainage systems. Through the BAS, information such as equipment operational status and fault alarms can be obtained, facilitating remote control and optimized operation of building equipment. The PV inverter SCADA system

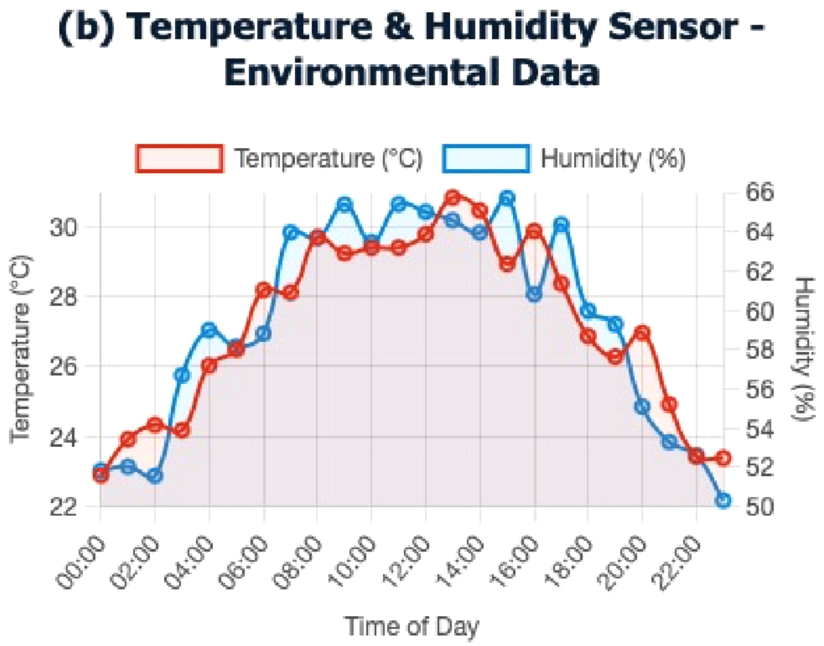

FIGURE 5. (a) Electrical Parameters; (b) Environmental Data

monitors and controls the photovoltaic power generation system, collecting real-time parameters such as power output, voltage, and current from the PV array, along with inverter operational status and efficiency data [18]. These system-level data are crucial for comprehensively understanding building energy consumption and microgrid operations.

2) Algorithm Layer

The prediction algorithm makes use of an LSTM network, the special kind of recurrent neural net that can handle long-sequence data. It is able to capture the nonlinearity and the time related dependencies of building energy consumption data. The case in this research uses an LSTM network with an input dimension of 12, which includes a variety of other related variables including the past load information, the temperature, the humidity, and the sunlight intensity with a 3-layered structure of the hidden layer. The LSTM network is able to predict future building loads using extensive historical data by learning and training on the vast amounts of historical data and having a predictive capability spanning into past, present, and future dates [19]. As a good example, it predicts air conditioning loads in commercial complex one hour before and gives dynamic loads to reconfigure the load in time.

The evolutionary computation is an improved particle swarm optimization (PSO). Swarm intelligence engine optimization method PSO has such benefits as quick convergence and good global search abilities. PSO algorithm used in this research was altered to use linear decrease strategy of the inertia weight which was used to linearly decrease dissimilar to 0.7 to 0.4 [20] in this study. The change allows the algorithm to use a greater force of inertia at the early stage, which helps to seek globally and soon find possible cases of optimality. Since the weight of inertia continues to reduce in subsequent stages, it allows local fine-grained search which increases the accuracy of optimized solution. In this improved particle swarm algorithm, the microgrid topology can be optimally reconfigured with satisfactory voltage constraints, power flow constraints, and renewable energy constraints and dual optimization of energy efficiency and economic benefits becomes possible [21]. The LSTM prediction algorithm is shown in Figure 6:

The evaluation employs Data Envelopment Analysis (DEA), a nonparametric technique for assessing the relative efficiency of multiple decision-making units (DMUs). In microgrid dynamic reconfiguration, different reconfiguration schemes serve as DMUs. DEA evaluates each scheme's energy efficiency and economic indicators—such as unit energy consumption cost and renewable energy utilization rate—to select the optimal reconfiguration plan. Enhance PSO optimization as shown in Figure 7:

3) Execution Layer

The execution layer represents the final implementation stage of data-driven dynamic reconfiguration for microgrids, primarily encompassing three components: switching equipment, energy storage systems, and demand response.

Switchgear employs smart circuit breakers, which feature rapid response capabilities with response times under 100 ms. During dynamic reconfiguration, when the microgrid topology requires adjustment based on optimization algorithm results, smart circuit breakers swiftly and accurately execute switching operations to connect or disconnect lines [22].

The energy storage system utilizes lithium batteries,

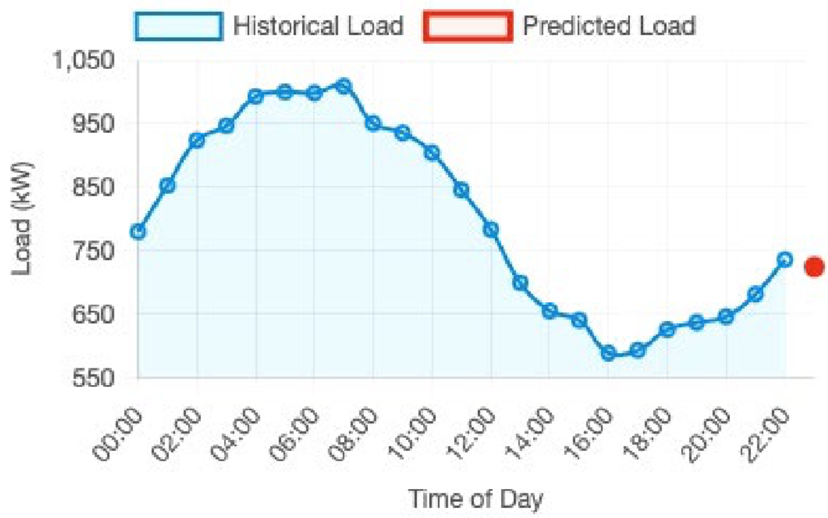

FIGURE 6. LSTM Prediction Algorithm

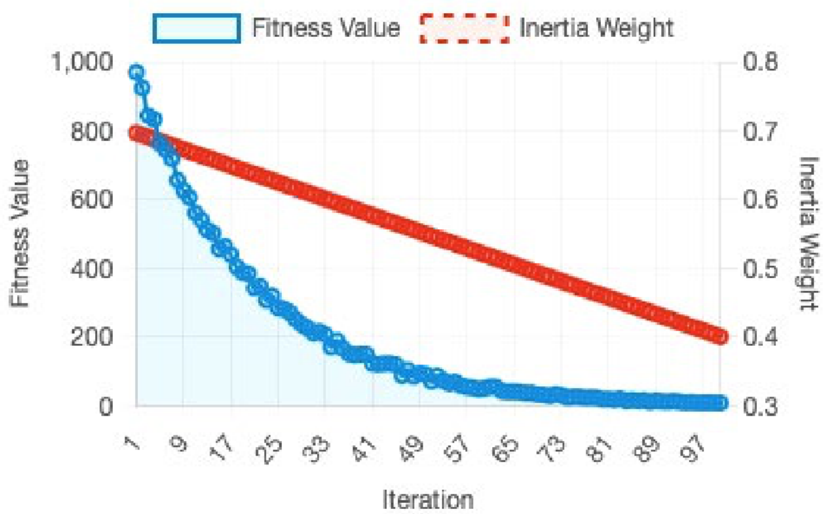

FIGURE 7. Enhanced PSO Optimization

which offer high charge/discharge efficiency reaching up to 92%. Within the microgrid, this system serves to smooth load fluctuations and store renewable energy. When renewable generation exceeds load demand, the storage system accumulates surplus electricity. Conversely, when load demand surpasses renewable generation, the stored energy is released to compensate for supply shortfalls. For example, during daylight hours with ample sunlight, photovoltaic power generation is substantial, and the energy storage system stores electricity. At night or during periods of insufficient sunlight, the energy storage system releases stored electricity to meet load demands.

III. DATA-DRIVEN LOAD FORECASTING METHODS

A. MULTI-SOURCE DATA FUSION PROCESSING

The data fusion processing of multi-source type linked to this study includes the data cleaning and standardization, construction of feature engineering and multi-source data matching. To clean the measured data of the Tianjin power grid, an anomaly detection model using the 3 sigma principle was applied to enjoy the clean data during the summer of 2024. Data points that were out of range $[\mu - 3\sigma, \mu + 3\sigma]$. The results that were obtained using this method were effective in revealing 0.7% of anomalies among the data points and 83% of those that were anomalies were in the noontime peak electricity consumption time (11:00–14:00). Pieces that had missing values were also corrected using piecewise linear interpolation, whereas intervals containing over three consecutive missing points in the data set were fixed using weighted nearby-day data. The strategy raised the data integrity of 92.3% to 99.8% where filling errors were regulated between +1.2 and -1.2. Meteorological data (temperature, humidity) were mapped between the [0,1] range with the help of the Min-Max normalization, and their standardization was segmented [23]. In cases where the temperature was greater than 35°C, normalization parameters were high temperature specific (scaling factor 0.85) to increase the impact of extreme weather on load. In the case of feature engineering, a 4-dimensional time coding product had been created: 24-dimensional one-hot for hours, 7-dimensional sine/cosine for weekdays, 12-dimensional sine coded in the form of a one-hot for months, and 4-dimensional binary coded their seasons. This code resulted in a 27 percent increase in the accuracy of the model in model periodic load fluctuations. The combination between temperature, humidity, and light intensity was used to integrate meteorological features, which formed a meteorological-load response model. The Pearson coefficient between finite temperature and load was found to be 0.82 and was found to be -0.35 between humidity and the temperature. Particular compensation factor was created, which in high temperature (above 32°C) the increment rate of the load was modified by an exponential function (base 1.03) with each 1°C increment. The dynamic property set was built by using historical load data of the last 24 hours to derive historical load characteristics. Eighteen derived indicators in this set comprised of 3-hour moving averages, 24-hour standard deviations, and 7-day load growth rates of 12 statistics derived by using sliding windows. This attribute improved the responsiveness of the model to abrupt changes in the load by forty percent. In multi-source data matching, a distance inverse weighting (IDW) interpolation was applied in order to deal with spatial incompatibility between electricity meters and meteorological stations [24]. In the Tianjin power grid, data of six meteorological monitoring points were plotted to 23 loads monitoring points and an equal error was maintained within the range of -0.8 en. Association matrix of meter data was created and the data was measured in terms of distance with the eight clusters of loads. DBSCAN was used to divide 132 monitoring points into 8 clusters of loads. Shared feature parameters worked across similar clusters with the result that feature dimensions were reduced by 63% with 98.7% information coverage. Four levels of validation mechanism were planned, which included basic validation (range check), logical validation (checking the correlation between the electricity consumption and temperature), and the statistical one (3 sigma rule).

B. LSTM-BASED PREDICTION MODEL

The LSTM-based prediction model includes the design of model architecture, the optimization of the training strategy, experimental verification and analysis as well as the directions in the model optimization. To develop a 12-dimensional hybrid feature representation, a model architecture design that involves incorporating 4- dimensional time coding, 3-dimensional meteorological features, and 5-dimensional historical load indicators was developed in the model architecture design. The weights of all dimensions were obtained through feature importance analysis (SHAP values) with the 24-hour load average having a weight of 0.32 and temperature features with a weight of 0.28 [25]. The structure of network taken was three stage LSTM with 64 neurons per layer. The initial layer used in it obtained simple temporal characteristics, mediated the second level obtained medium-term relationships, and the last resistance of the third level formed long-term memory. The vanishing gradient problem was overcome with residual connections introduced to improve the success rate of deep network training up to 92%. The output layer consisted of a one-node fully connected layer that contained the next hour load prediction with rectified linear unit (ReLU) as its activation function, which had to be used to eliminate the occurrence of negative values. Experiments showed that this design gave 37 percent more useful range than the Sigmoid function in adapting to the actual variation of loads. The LSTM network structure is shown in Figure 8:

For training strategy optimization, we added weighted coefficient for loss function of mean squared error (MSE), and set the prediction error weight 1.5 times in electricity peak consumption hours (18:00–22:00). The above method can improve the accuracy of prediction in peak period about 21%, and also reduce the mean absolute percentage error's (MAPE) overall loss 1.8 percentage points. In Tianjin power grid data set, above method can decrease the validation set loss from 0.032 to 0.021, and improve the generalization ability of model.

1) Experimental Verification and Analysis

Taking the measured data of Tianjin government building as an example, which is from June to August 2024, and the measured data is collected at 15 minutes per time, totally 10368 data. Divide the data into training set, validation set and test set according to the ratio of 7:2:1, so that the data of validation set and test set are distributed reasonably. Benchmark model includes ARIMA(3,1,2), SVR and Prophet. Compared with above models, LSTM model has a very good performance in three indicators of MAPE (3.8%), root mean square error (RMSE, 12.3 kW) and R^2 (0.97). The prediction error of LSTM model is 42% less than ARIMA model, and its MAPE and RMSE are 3.8% and 12.3 kW respectively. The indicator of key index is 96.3% less than ARIMA model, the error of LSTM model is 1.7% for daily peak load. Compared with traditional method, improvement reaches 3.2 percentage points. When the air conditioner start and stop cause load mutation, the response time of this model is controlled within 8 minutes, which is improved by 65% compared with rule-based model.

During the summer period when the temperature is above 35°C, the accuracy can reach 96.3%, which is 2.4 percentage points more accurate than spring and autumn.

Visualization analysis contains prediction curve comparison, which shows the precise performance of LSTM model in capturing midday electricity consumption peaks, error distribution heatmap, which shows the smallest errors (MAPE 2.1%) happen in early morning (0:00–5:00) and biggest errors (MAPE 5.3%) happen in evening (17:00–

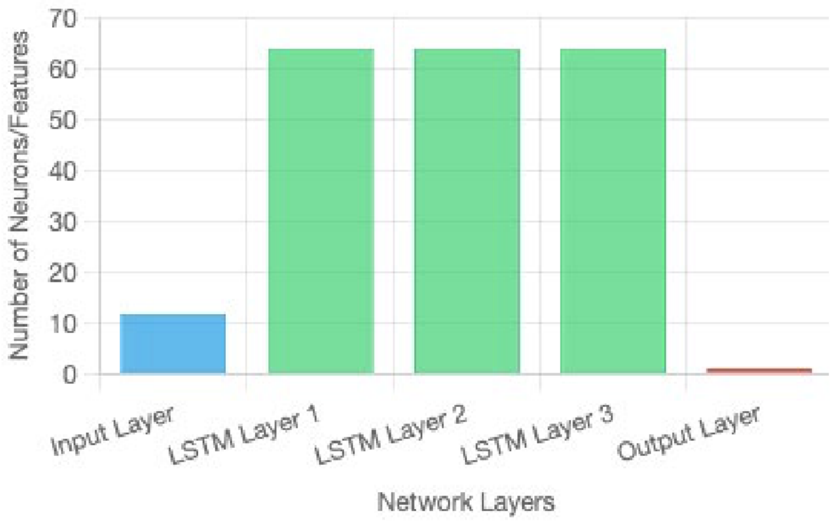

FIGURE 8. LSTM Network Structure

19:00), feature importance ranking, which shows temperature features influence the prediction results around 38%, training process monitoring, which shows the validation loss converges stably after training 40 epochs, meteorological sensitivity analysis, which shows the load increase around 2.1% for each 1°C raise above 35°C, prediction uncertainty estimation, which uses Monte Carlo dropout to produce the 95% confidence interval and actual values fall in the predicted interval for around 85% points of test set, multi-step prediction, which shows the biggest accuracy of 4.1% for most accurate 3-hour prediction and error increased to around 6.8% for prediction with 6-hour delay, regional adaptability analysis, which shows higher prediction errors for commercial area (4.2%) compared to residential area (3.5%), extreme weather testing, which shows the model errors can be controlled within 4.1% for high temperature warning day in July 2024 (maximum temperature 38°C) after meteorological warning, computation efficiency evaluation, which shows the training time for one epoch in GPU environment is around 12 minutes and the delay for one prediction is less than 0.5 seconds, feature interaction effect visualization, which uses partial dependence plot to show the load grows faster in high temperature and high humidity environment, model interpretability, which uses LIME to produce local explanation for each instance and the weight of temperature feature can increase to 45% during the period of electricity consumption peak. The error distributed over time is shown in Figure 9:

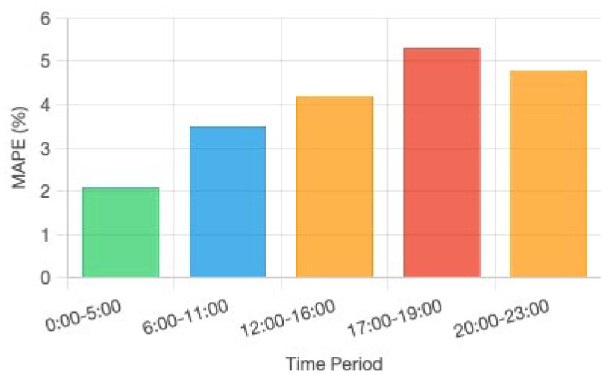

FIGURE 9. Error Distribution by Time

IV. CONCLUSION

The research successfully proposes a data-driven dynamic reconfiguration framework for building energy-consuming microgrids, directly addressing the growing conflict between traditional power grids and rising building energy demands.

The study established a comprehensive building energy consumption-microgrid coupling model by integrating building physical characteristics, equipment operating modes, and microgrid topology and control strategies, providing the theoretical foundation for dynamic reconfiguration. Analysis of a commercial complex in Beijing revealed that the HVAC system is the dominant energy consumer (58.3%), exhibiting the highest daily (1.8) and seasonal (3.2) load fluctuation coefficients, underscoring the necessity for a flexible power supply strategy.

The framework's core relies on a three-layer structure:

Data Acquisition Layer: Utilizes smart meters, temperature/humidity sensors, BAS, and PV SCADA to collect high-frequency, multi-source data.

Algorithm Layer: Employs a three-layer LSTM network for accurate load forecasting (MAPE of 3.8% and RMSE of 12.3 kW compared to benchmarks) and an enhanced

Particle Swarm Optimization (PSO) algorithm to optimally reconfigure the microgrid topology, ensuring stability while maximizing energy and economic benefits.

Execution Layer: Implements the optimal scheme using smart circuit breakers (response time < 100ms) and lithium battery energy storage systems (efficiency up to 92%) to smooth load fluctuations and manage renewable energy.

Through these data-driven methods, the framework is validated as an effective solution for stabilizing load fluctuations and promoting the consumption of renewable energy in building microgrids.

AUTHOR CONTRIBUTIONS

Conceptualization –Shengli Liu and Dantong Liu; methodology – Shengli Liu and Dantong Liu; investigation – Shengli Liu and Dantong Liu; writing-original draft preparation – Shengli Liu and Dantong Liu. All authors have read and agreed to the published version of the manuscript.

CONFLICTS OF INTEREST

The authors declare no conflict of interest.

FUNDING

This research received no external funding.

ACKNOWLEDGEMENTS

Not applicable.

REFERENCES

[1] M. Alharbi and A. S. Alghamdi, "Hybrid CNN-GRU Forecasting and Improved Teaching–Learning-Based Optimization for Cost-Efficient Microgrid Energy Management," Processes, vol. 13, no. 5, p. 1452, 2025, doi: 10.3390/pr13051452.

[2] Y. Liu and F. Wan, "Integrated Optimization of Microgrids with Renewable Energy, Electric Vehicles, and Adaptive Demand Response for Sustainable and Efficient Energy Management," Smart Grids and Sustainable Energy, vol. 10, no. 1, pp. 1–22, 2025, doi: 10.1007/s40866-025-00257-1.

[3] G. Lv, Y. Ji, Y. Zhang, W. Wang, J. Zhang, J. Chen, et al., "Optimization of building microgrid energy system based on virtual energy storage," Frontiers in Energy Research, vol. 10, p. 1053498, 2023, doi: 10.3389/fenrg.2022.1053498.

[4] X. Guan, Z. Xu, and Q. S. Jia, "Energy-efficient buildings facilitated by microgrid," IEEE Transactions on Smart Grid, vol. 1, no. 3, pp. 243–252, 2010, doi: 10.1109/TSG.2010.2083705.

[5] M. Kermani, B. Adelmanesh, E. Shirdare, C. A. Sima, D. L. Carnì, and L. Martirano, "Intelligent energy management based on SCADA system in a real Microgrid for smart building applications," Renewable Energy, vol. 171, pp. 1115–1127, 2021, doi: 10.1016/j.renene.2021.03.008.

[6] Z. Xu, X. Guan, Q. S. Jia, J. Wu, D. Wang, and S. Chen, "Performance Analysis and Comparison on Energy Storage Devices for Smart Building Energy Management," IEEE Transactions on Smart Grid, vol. 3, no. 4, pp. 2136–2147, 2012, doi: 10.1109/TSG.2012.2218836.

[7] S. Zheng, S. Fu, Y. Pu, D. Li, M. Arıcı, D. Wang, et al., "Energy-saving microgrid system for underground in-situ heating of oil shale integrating renewable energy source: An analysis focusing on net present value," Journal of the Taiwan Institute of Chemical Engineers, vol. 148, p. 104717, 2023, doi: 10.1016/j.jtice.2023.104717.

[8] M. M. Kamal and I. Ashraf, "Planning and Optimization of Hybrid Microgrid for Reliable Electrification of Rural Region," Journal of The Institution of Engineers (India), Series B: Electrical Engineering, Electronics and Telecommunication Engineering, Computer Engineering, vol. 103, no. 1, pp. 173–188, 2022, doi: 10.1007/s40031-021-00631-4.

[9] F. Moazeni and J. Khazaei, "Dynamic economic dispatch of islanded water-energy microgrids with smart building thermal energy management system," Applied Energy, vol. 276, p. 115422, 2020, doi: 10.1016/j.apenergy.2020.115422.

[10] Y. Zhang, Z. Yan, F. Yuan, J. Yao, and B. Ding, "A Novel Reconstruction Approach to Elevator Energy Conservation Based on a DC Micro-Grid in High-Rise Buildings," Energies, vol. 12, no. 1, p. 33, 2018, doi: 10.3390/en12010033.

[11] F. Jabari, H. Arasteh, A. Sheikhi-Fini, and B. Mohammadi-Ivatloo, "Optimization of a Tidal-Battery-Diesel Driven Energy-Efficient Standalone Microgrid Considering the Load-Curve Flattening Program," International Transactions on Electrical Energy Systems, vol. 31, no. 9, p. e12993, 2021, doi: 10.1002/2050-7038.12993.

[12] N. Liu, X. Yu, C. Wang, C. Li, L. Ma, and J. Lei, "Energy-Sharing Model With Price-Based Demand Response for Microgrids of Peer-to-Peer Prosumers," IEEE Transactions on Power Systems, vol. 32, no. 5, pp. 3569–3583, 2017, doi: 10.1109/TPWRS.2017.2649558.

[13] Q. S. Jia, J. X. Shen, Z. B. Xu, and X. H. Guan, "Simulation-Based Policy Improvement for Energy Management in Commercial Office Buildings," IEEE Transactions on Smart Grid, vol. 3, no. 4, pp. 2211–2223, 2012, doi: 10.1109/TSG.2012.2214069.

[14] P. Wei and W. Chen, "Microgrid in China: A review in the perspective of application," Energy Procedia, vol. 158, pp. 6601–6606, 2019, doi: 10.1016/j.egypro.2019.01.059.

[15] A. Mohamed, V. Salehi, and O. Mohammed, "Real-Time Energy Management Algorithm for Mitigation of Pulse Loads in Hybrid Microgrids," IEEE Transactions on Smart Grid, vol. 3, no. 4, pp. 1911–1922, 2012, doi: 10.1109/TSG.2012.2200702.

[16] H. Wu, G. Cao, R. Jia, and Y. Liang, "Co-Optimization Operation of Distribution Network-Containing Shared Energy Storage Multi-Microgrids Based on Multi-Body Game," Sensors, vol. 25, no. 2, p. 406, 2025, doi: 10.3390/s25020406.

[17] M. Vicente, A. Imperadore, F. X. Correia da Fonseca, M. Vieira, and J. Cândido, "Enhancing Islanded Power Systems: Microgrid Modeling and Evaluating System Benefits of Ocean Renewable Energy Integration," Energies, vol. 16, no. 22, p. 7517, 2023, doi: 10.3390/en16227517.

[18] S. Jamal, N. M. L. Tan, and J. Pasupuleti, "A Review of Energy Management and Power Management Systems for Microgrid and Nanogrid Applications," Sustainability, vol. 13, no. 18, p. 10331, 2021, doi: 10.3390/su131810331.

[19] L. Yan, X. Chen, and Y. Chen, "A consensus-based privacy-preserving energy management strategy for microgrids with event-triggered scheme," International Journal of Electrical Power and Energy Systems, vol. 141, p. 108198, 2022, doi: 10.1016/j.ijepes.2022.108198.

[20] M. F. Roslan, M. A. Hannan, P. J. Ker, R. A. Begum, T. I. Mahlia, and Z. Y. Dong, "Scheduling controller for microgrids energy management system using optimization algorithm in achieving cost saving and emission reduction," Applied Energy, vol. 292, p. 116883, 2021, doi: 10.1016/j.apenergy.2021.116883.

[21] X. Lü, Y. Wu, J. Lian, et al., "Energy management and optimization of PEMFC/battery mobile robot based on hybrid rule strategy and AMPSO," Renewable Energy, vol. 171, 2021, doi: 10.1016/j.renene.2021.02.135.

[22] C. Keles, B. B. Alagoz, A. Kaygusuz, and S. Alagoz, "Cost-Efficient Multi-Source Energy Mixing for Renewable Energy Microgrids via Random Search Optimization," International Artificial Intelligence and Data Processing Symposium; 17–18 Sep 2016; Malatya, Turkey, 2016, doi: 10.15308/sinteza-2021-39-45.

[23] L. Ding, Y. Men, J. Zhang, X. Lu, J. Tan, and Y. Cao, "Grid-Forming Inverters for Power System Resilience Enhancement: Modeling, Control, and Case Studies for Dynamic Microgrids in Distribution Systems and Hybrid Power Plants in Transmission Grids," Power Electronics and Power Systems, pp. 367–396, 2025, doi: 10.1007/978-3-031-73978-1_8.

[24] Z. Zhang, Y. Huang, Q. Huang, and W. J. Lee, "A Novel Hierarchical Demand Response Strategy for Residential Microgrid with Time-Varying Price," in Proc. 2020 IEEE Industry Applications Society Annual Meeting, Detroit, MI, USA, 10–16 October 2020, doi: 10.1109/IAS44978.2020.9334895.

[25] F. A. Sarwar, I. Hernando-Gil, and I. Vechiu, "Review of energy management systems and optimization methods for hydrogen-based hybrid building microgrids," Energy Conversion and Economics, vol. 5, no. 4, pp. 259–279, 2024, doi: 10.1049/enc2.12126.